

# Copper Oxide Films Grown by Atomic Layer Deposition from Bis(tri-*n*-butylphosphane)-copper(I)acetylacetonate on Ta, TaN, Ru, and SiO<sub>2</sub>

Thomas Waechtler<sup>||</sup>, Steffen Oswald<sup>†</sup>, Nina Roth<sup>‡</sup>, Alexander Jakob<sup>‡</sup>, Heinrich Lang<sup>‡</sup>, Ramona Ecke\*, Stefan E. Schulz<sup>\*§</sup>, Thomas Gessner<sup>\*§\*\*</sup>, Anastasia Moskvina<sup>¶</sup>, Steffen Schulze<sup>¶</sup>, and Michael Hietschold<sup>¶</sup>

\*Center for Mircotechnologies (ZfM), Chemnitz University of Technology, D-09107 Chemnitz, Germany

<sup>†</sup>Leibniz Institute for Solid State and Materials Research (IFW), D-01069 Dresden, Germany

<sup>‡</sup>Department of Inorganic Chemistry, Institute of Chemistry, Chemnitz University of Technology, D-09107 Chemnitz, Germany

<sup>§</sup>Fraunhofer Research Institution for Electronic Nano Systems (ENAS), D-09126 Chemnitz, Germany

<sup>¶</sup>Solid Surfaces Analysis and Electron Microscopy Group, Institute of Physics, Chemnitz University of Technology, D-09107 Chemnitz, Germany

<sup>||</sup>E-mail: thomas.waechtler@zfm.tu-chemnitz.de

\*\*Electrochemical Society Active Member.

© The Electrochemical Society, Inc. 2009. All rights reserved. Except as provided under U.S. copyright law, this work may not be reproduced, resold, distributed, or modified without the express permission of The Electrochemical Society (ECS). The archival version of this work was published in *Journal of The Electrochemical Society*, Vol. 156, No. 6, pp. H453–H459 (2009), ISSN 0013-4651, Digital Object Identifier (DOI): 10.1149/1.3110842 (<http://dx.doi.org/10.1149/1.3110842>).

**Abstract**—The thermal atomic layer deposition (ALD) of copper oxide films from the non-fluorinated yet liquid precursor bis(tri-*n*-butylphosphane)copper(I)acetylacetonate, [(*n*-Bu<sub>3</sub>P)<sub>2</sub>Cu(acac)], and wet O<sub>2</sub> on Ta, TaN, Ru and SiO<sub>2</sub> substrates at temperatures of <160°C is reported. Typical temperature-independent growth was observed at least up to 125°C with a growth-per-cycle of ~0.1 Å for the metallic substrates and an ALD window extending down to 100°C for Ru. On SiO<sub>2</sub> and TaN the ALD window was observed between 110 and 125°C, with saturated growth shown on TaN still at 135°C. Precursor self-decomposition in a chemical vapor deposition mode led to bimodal growth on Ta, resulting in the parallel formation of continuous films and isolated clusters. This effect was not observed on TaN up to about 130°C and neither on Ru or SiO<sub>2</sub> for any processing temperature. The degree of nitridation of the tantalum nitride underlayers considerably influenced the film growth. With excellent adhesion of the ALD films on all substrates studied, the results are a promising basis for Cu seed layer ALD applicable to electrochemical Cu metallization in interconnects of ultralarge-scale integrated circuits.

## I. INTRODUCTION

WHILE copper is now widely accepted as conductor material for interconnect systems of ultralarge-scale integrated circuitry (ULSI) [1], there is an increasing need for extremely thin, continuous Cu films that are conformal in demanding nanoscale geometries. The conventional damascene technology applied for creating the metallization system of ULSI devices requires Cu seed layers as starting point for electrochemical Cu filling (ECD) of vias and conductor lines embedded in patterned SiO<sub>2</sub> or low-*k* / ultra low-*k* material [1], [2]. So far sputtering is the method of choice for depositing such seed layers, but with reduced line width and increasing aspect ratio of the interconnect features this method tends to fail due to its inherent non-conformal deposition characteristic as schematically shown in Fig. 1.

Gas-phase chemical deposition methods, such as chemical vapor deposition (CVD) and atomic layer deposition (ALD), are being discussed as alternative methods in this respect [3]–[6]. ALD, in particular, is a viable technique to obtain contin-

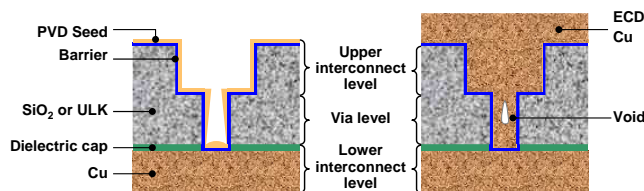


Fig. 1. Schematic of Cu ULSI dual damascene metallization: Especially in high-aspect-ratio features, such as vias, the sputtered PVD seed layer is prone to nonconformalities (left), which may result in the formation of voids during the subsequent electrochemical Cu deposition (right).

uous, ultrathin films with very good step coverage in extreme geometries and on three-dimensional nanoscale objects due to the self-limiting film growth behavior [7], [8].

As ALD relies on the reaction of a chemisorbed monolayer of a metal precursor with a co-reactant to form the desired material, a suitable precursor combination must be found. In contrast to ALD processes of noble metals, where also oxidizing agents can be used to obtain metal films [9]–[15], metallic copper films are only accessible by ALD directly when the Cu precursor is reduced. This can be accomplished by plasma-enhanced ALD (PEALD) with atomic hydrogen as the reducing agent [16]–[18]. However, these approaches deteriorate ALD's ability to conformally coat complex geometries, because especially hydrogen plasmas tend to deplete down in nanoscale trenches and shadowed areas. As a consequence, this leads to reduced step coverage and non-conformal film growth, compromising a major advantage inherent to ALD. From this point of view, thermal ALD is generally favored.

Pure thermal approaches to form metallic Cu have been proposed with  $[\text{CuCl}]$  and  $\text{H}_2$  as the precursors, requiring elevated processing temperatures between 360 and 425°C [19]–[21]. These processes yielded isolated Cu clusters only; due to the strong agglomeration tendency Cu exhibits especially on substrates like silica, refractory metals or refractory metal nitrides [22]–[27]. Therefore such processes are problematic for applications where ultra-thin, continuous films are required. In addition, the use of solid precursors with high melting points such as metal halides further complicates the situation as the precursors must be sublimed in situ, making it cumbersome to guarantee a constant and reproducible precursor flow rate which is indispensable for reproducible processes applicable to mass production.

Using metal-organic precursors, in contrast, lower sublimation temperature, or in many cases precursor liquid delivery or bubbling as well as reduced processing temperatures are possible. In this respect, Cu(II)  $\beta$ -diketonates have been studied. With copper(II) hexafluoroacetylacetonate,  $[\text{Cu}(\text{hfac})_2]$ , ALD was reported from 230°C [28], [29]. Although fluorinated precursors exhibit the advantage of greater volatility compared to their non-fluorinated counterparts, adhesion problems of the deposited films have been observed as a result from fluorine-containing residues accumulating at the interface to the substrate in Cu CVD processes from  $[(\text{TMVS})\text{Cu}(\text{hfac})]$  (CupraSelect) (TMVS = trimethylvinylsilane) [30]–[32]. As an alternative, ALD was studied using the non-fluorinated copper(II) tetramethylheptanedionate,  $[\text{Cu}(\text{thd})_2]$ , and direct

reduction to form Cu. However, these processes turned out to be highly substrate-dependent, as film growth relied on catalytic underlayers such as Pt or Pd [33], [34].

Apart from Cu(II) precursors, Cu(I) amidinates have recently been reported to react with hydrogen already at temperatures  $\leq 200^\circ\text{C}$  to give copper films by ALD [35]–[37]. However, most of these precursors are solids under standard conditions. Furthermore, smooth and continuous ALD Cu films are only obtained on metallic nucleation layers such as Co or Ru, while discontinuous islands grow on materials like  $\text{WN}_x$  [38], [39]. With respect to a practical application, such requirements would result in rather complex processes.

To circumvent these issues associated with direct precursor reduction for growing metallic Cu films, alternatives are being discussed with respect to simple hence cost-effective processes. CVD and ALD approaches include the formation of films of copper compounds such as nitrides [40]–[42] or oxides [28], [29], [43]–[47] which are subsequently reduced. In this respect, we here investigate the ALD of oxidic copper films from bis(tri-*n*-butylphosphane)copper(I)acetylacetonate,  $[(^n\text{Bu}_3\text{P})_2\text{Cu}(\text{acac})]$  ( $^n\text{Bu}$  = *n*-butyl) for the first time. This liquid, non-fluorinated Cu(I)  $\beta$ -diketonate precursor is accessible by a straight-forward synthesis methodology from inexpensive educts. Hence it also appears attractive for later large-scale industrial application at reasonable cost. In our current study, we concentrate on pure thermal ALD processes to eliminate the drawbacks of PEALD associated with reduced film conformality in high aspect ratio features. For similar reasons and also in order to avoid extensive oxidation of substrate materials as well as the use of costly equipment, ozone-based oxidation processes are not investigated. Rather, a mixture of water vapor and oxygen ("wet oxygen") is used as oxidizing agent during ALD. With the target application of seed layers for ULSI damascene metallization in mind, ALD was carried out on tantalum as well as tantalum nitride diffusion barrier layers. Ruthenium, as a candidate for Cu nucleation layers [12], [48], [49] and potential component of advanced diffusion barrier systems [50]–[55], was also used as substrate. For comparison to the conductive substrates, depositions were further carried out on  $\text{SiO}_2$ .

## II. EXPERIMENTAL

### A. Precursor Considerations

Bis(tri-*n*-butylphosphane)copper(I)acetylacetonate,  $[(^n\text{Bu}_3\text{P})_2\text{Cu}(\text{acac})]$  (Fig. 2) was synthesized under inert gas atmosphere by published methods [56], [57].

Under standard conditions, the precursor is a pale yellow liquid and can be stored in inert gas atmosphere for months without decomposition. Vapor pressure measurements show that the precursor has a vapor pressure of 0.02 mbar at 98°C (Fig. 3), being comparable to  $[\text{Cu}(\text{acac})_2]$  but considerably lower than fluorinated substances such as  $[(\text{TMVS})\text{Cu}(\text{hfac})]$  or  $[\text{Cu}(\text{hfac})_2]$  [58]–[60]. However, for ALD a high vapor pressure is not as critical as for CVD where high deposition rates are desirable. Since ALD relies on forming a chemisorbed monolayer of precursor molecules on a substrate, also less-volatile liquids can be applied to ALD.

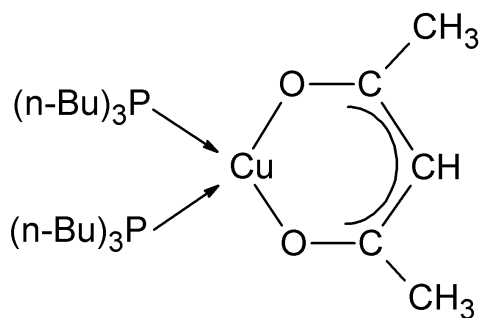


Fig. 2. Structure of  $[(n\text{-Bu}_3\text{P})_2\text{Cu}(\text{acac})]$  (molecular weight: 567.3 g/mol).

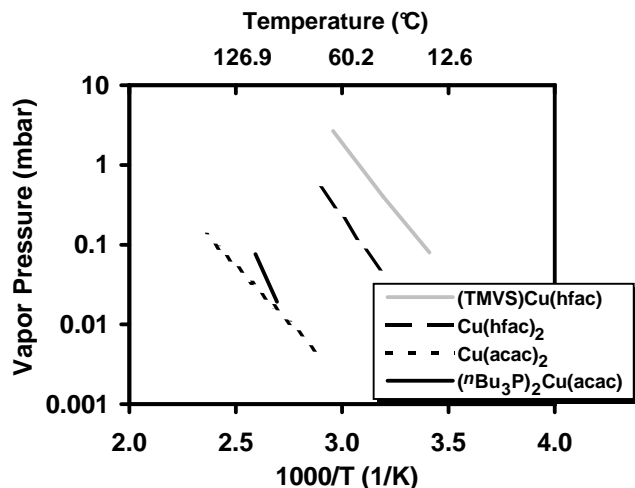


Fig. 3. Vapor pressure data for  $[(n\text{-Bu}_3\text{P})_2\text{Cu}(\text{acac})]$  compared to other commonly used Cu CVD/ALD precursors [58]–[60].

In a previous report [57], Cu CVD by thermal disproportionation was shown at 220°C with this precursor. As differential scanning calorimetric studies (DSC) of the molecule showed major decomposition peaks only at 237 and 255°C [57], we chose the precursor as a viable candidate for low-temperature ALD studies.

### B. ALD Experiments

ALD experiments were carried out in a cold-wall, 4 in. single-wafer vertical flow reactor equipped with a load-lock chamber [61], [62]. The process control system of the original CVD reactor had been modified to enable automated, cyclic processing [63]. The deposition chamber was evacuated with a combination of a turbomolecular and a roots pump, both backed with rotary pumps, to achieve a base pressure of  $<3 \times 10^{-6}$  mbar. The ALD processes themselves were carried out at pressures between 0.8 and 1.5 mbar. During deposition, the chamber walls were kept at 85°C to avoid precursor condensation. Each ALD cycle consisted of the steps summarized in Table I. Due to the large reactor volume of nearly 13 liters, relatively long pulses were necessary both to reach saturation of the precursor chemisorption as well as to guarantee sufficient purging of the chamber.

TABLE I  
STEPS OF AN ALD CYCLE.

Step	Description	Pulse length (s)
1	Precursor exposure	3–5
2	Argon purging	5
3	Oxidation (oxygen + water vapor)	7–11
4	Argon purging	5

The copper precursor was stored at room temperature under Ar atmosphere in a stainless steel stock bottle. During processing it was evaporated by a Bronkhorst liquid delivery system (LDS) with Ar as carrier gas (flow rate  $\sim 700$  sccm). This approach avoids exposing the precursor stock to heat and thus leads to a longer shelf life of the substance. After evaporating between 85 and 100°C at a flow rate of 10 to 20 mg/min and mixing with carrier gas, the precursor vapor was transported to the deposition chamber via heated stainless steel tubes. Water vapor was generated by a bubbler, also using Ar as carrier gas, at a temperature of 45 to 50°C. With an Ar flow of 200 sccm, approximately 18 to 20 mg/min H<sub>2</sub>O were evaporated. In parallel to the water vapor, 90 sccm of oxygen were flown during the oxidation pulses. The purging steps were realized by supplying 145 sccm of Ar. The 4 in. wafers that were used as substrates were heated resistively by a graphite heater during the ALD. The processing temperature ranged from 100 to 155°C. As starting layers, 40 nm of TaN or combinations with Ta (Ta/TaN, i.e., 20 nm Ta on top of 20 nm TaN), the preferred diffusion barrier system for ULSI Cu interconnects, were sputtered onto the Si prior to the ALD processes. The sputtering was realized in a Balzers CLC 9000 equipment. The Ta/TaN stacks were formed in continuous processes by turning off the N<sub>2</sub> flow when the desired TaN thickness was reached. Because of this, a continuous transition was obtained from TaN to Ta, and in some cases the Ta was also unintentionally nitrated. Si substrates coated with 100 nm Ru on top of a 10 nm Ti adhesion layer, both prepared by evaporation, were purchased from Advantiv Technologies, Inc., Fremont, CA (USA) and used as received. For depositions on silica, 4 in. Si wafers were thermally oxidized in a Centrotherm tube furnace prior to the ALD processes. All substrates were exposed to air before the ALD and were not pretreated in situ.

### C. Sample Characterization

The surface structure and morphology of the ALD films was studied by field-emission scanning electron microscopy (SEM) on a LEO 982 Digital Scanning Microscope as well as atomic force microscopy (AFM) with a Digital Instruments NanoScope IIIa in tapping mode using standard silicon tips. Spectroscopic ellipsometry with a SENTECH SE 850 ellipsometer was applied to determine the thickness of the ALD films. Selected samples were studied in more detail by cross-sectional transmission electron microscopy (TEM) with respect to the film structure as well as to verify the thickness values obtained from ellipsometry. A Philips CM20 TEM equipped with a field-emission gun was used for these investigations. Additionally, electron energy loss spectroscopy (EELS) and electron diffraction analyses were carried out

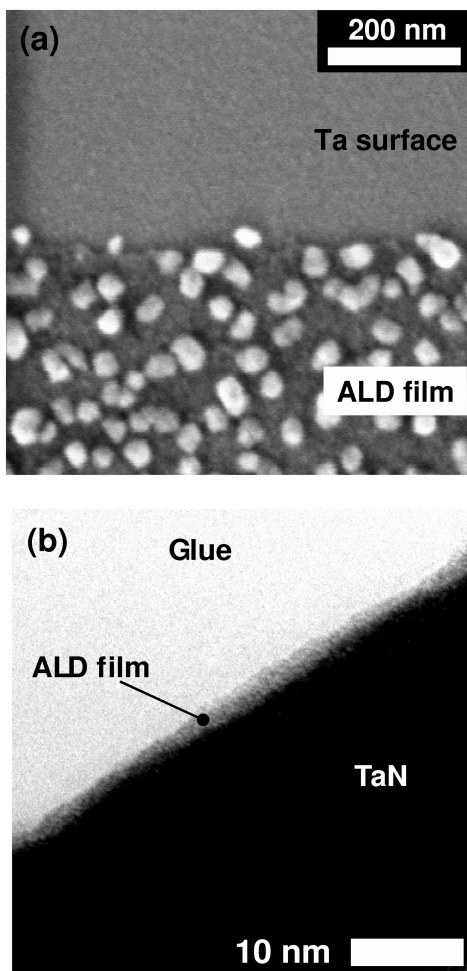


Fig. 4. (a) Top-view SEM image of a Cu/Cu<sub>x</sub>O ALD film on Ta grown at 135°C. The film was partially etched to expose the Ta surface. The bimodal growth characteristic has led to cluster formation in parallel to the growth of a continuous film. (b) Cross-sectional TEM image of a perfect ALD film grown on TaN at 125°C. No clusters are visible. By spectroscopic ellipsometry, a film thickness of 3.6 nm was determined.

on this TEM. Chemical analysis of the samples was further realized by X-ray photoelectron spectroscopy (XPS) on a PHI 5600 (Physical Electronics) with Al K<sub>α</sub> X-rays (1486.7 eV) used for excitation. The adhesion of the films was examined with the tape test using Tesa 4129 tape with an adhesion force of 8 N per 25 mm.

### III. RESULTS AND DISCUSSION

For the ALD experiments carried out on Ta a bimodal growth characteristic was experienced, leading to the parallel formation of continuous films and separated islands. In an earlier report [64], it was already shown that when using wet oxygen rather than only O<sub>2</sub> or water vapor during the ALD much better results can be obtained, which is due to the enhanced oxidizing activity of the H<sub>2</sub>O/O<sub>2</sub> combination. Fig. 4a shows a top-view SEM image of a Ta sample where the ALD film has been partially etched away. Between the clusters, a continuous film can be seen. On TaN, in contrast, continuous films without any larger aggregates were obtained up to 125°C (Fig. 4b).

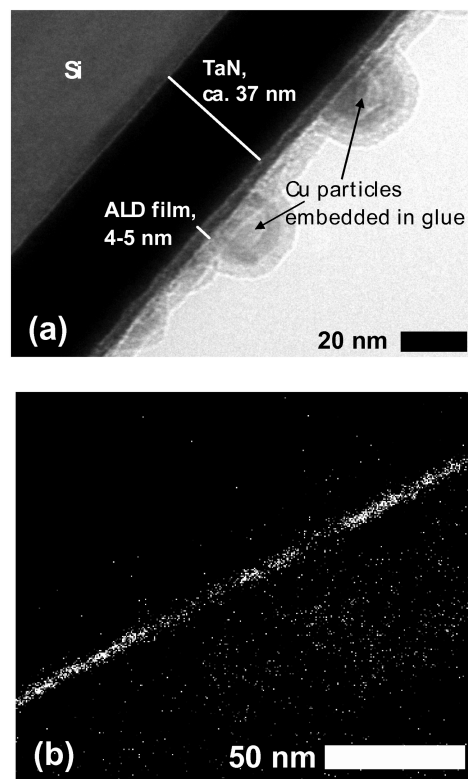


Fig. 5. (a) Cross-sectional TEM image of an ALD film grown on TaN at 135°C. Besides a continuous film of ~5 nm thickness (ellipsometry: 4.9 nm), clusters of a size between 15 and 20 nm are visible. (b) EELS map for Cu of the same sample.

For ALD films grown at 135°C, very small clusters in the range of 15 to 20 nm were detected by cross-sectional TEM imaging (Fig. 5). With increasing temperature, however, larger clusters started to appear on TaN, too. Together with an increase in the growth per cycle (GPC), this points to self-decomposition of the precursor setting in. In fact, it was shown theoretically by Machado et al. [65], [66] that especially Ta is very reactive toward metal-organic precursors, causing them to decompose and even form fragments of the ligands. As that study further points out, this effect is much less pronounced on TaN surfaces. Apparently this results in a much better controlled ALD growth on TaN than on metallic Ta in the current experiments. This is also expressed by the self-saturated growth regime obtained on TaN at 135°C as reported before [64], although a slight increase in the GPC due to beginning CVD effects is already experienced at this temperature. The respective graph is reprinted here in Fig. 6. The growth characteristic for this process shown in Fig. 7 displays a linear behavior with increasing number of ALD cycles in the lower range, while for more than about 200 cycles, the data suggest a steeper increase. We believe this to be due to a change in the surface chemistry once the substrate gets completely covered with the growing film.

Fig. 8 displays XPS data of the Cu 2p<sub>3/2</sub> core level and the Cu LMM Auger transition for ALD films on TaN. The samples were fabricated at different processing temperatures both on stoichiometric and Ta-rich TaN. XPS analyses carried out approximately 40 days after deposition as well as 100

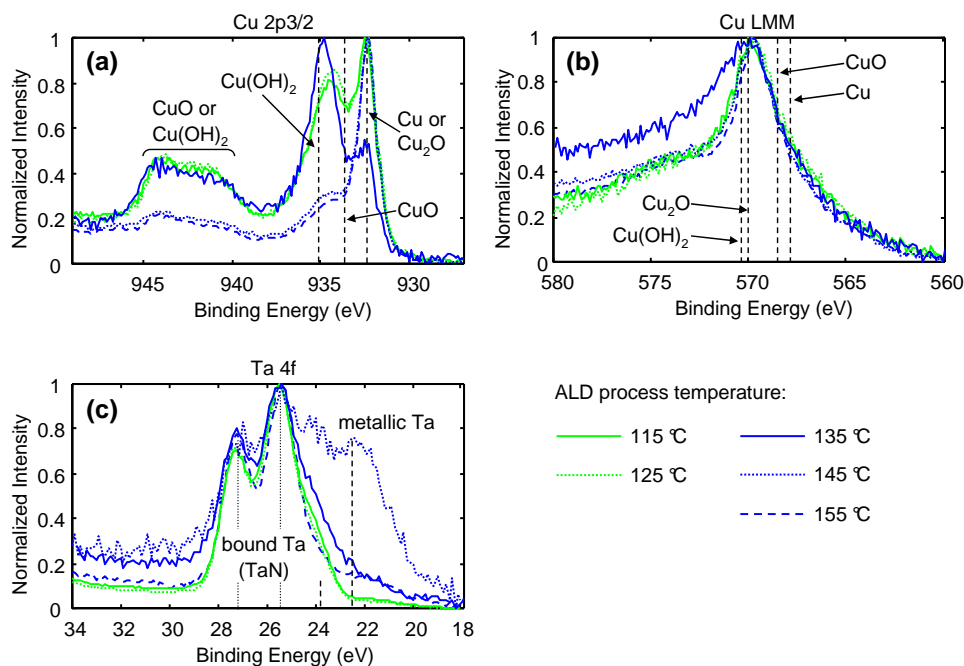


Fig. 8. XPS core level spectra of (a) Cu 2p<sub>3/2</sub> and (c) Ta 4f as well as binding energy data obtained for the Cu LMM Auger transition (b) from ALD samples on TaN. The processes of 400 cycles were carried out with precursor and purging steps of 5 s and 11 s oxidation pulses at 115, 125, 135, 145, and 155°C.

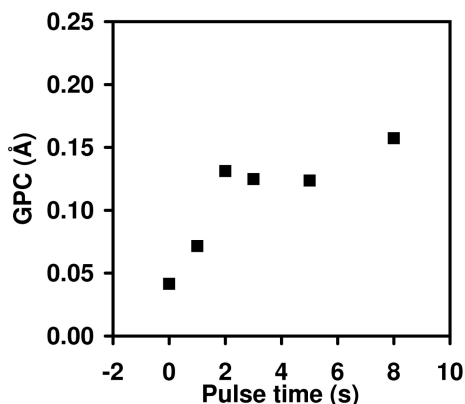


Fig. 6. GPC as a function of precursor pulse length for ALD on TaN at 135°C. Reprinted with permission from Ref. [64].

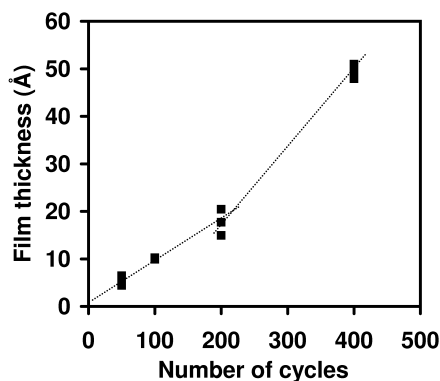


Fig. 7. Evolution of film thickness for ALD on TaN at 135°C with respect to the number of cycles, based on ALD runs according to Table I with 5 s precursor and 11 s oxidation pulses, separated by 5 s purging pulses. (The dotted lines are drawn to guide the eye.)

days later reveal that there is a general tendency of Cu<sub>2</sub>O formation, which is in accordance with other reports where preferably Cu(I) oxide was produced from [Cu(hfac)<sub>2</sub>] [45], [67] or [Cu(acac)<sub>2</sub>] [46] and H<sub>2</sub>O or H<sub>2</sub>O<sub>2</sub>. This is shown by the Cu 2p<sub>3/2</sub> peak (Fig. 8 a) at about 932.4 eV [68]. However, because this signal could also be assigned to metallic Cu [68], [69], one has to take into account the Auger spectra for the Cu LMM transition (Fig. 8 b) as well. There Cu would be expected at a binding energy of 567.7 to 567.9 eV [69], [70] while Cu<sub>2</sub>O should give a signal at 570 eV [68], [69]. [We note that, in Refs. [68]–[70], the kinetic energy of the Auger electrons is given, while in the current study we report the binding energy, i.e., the difference of the X-ray excitation energy and the kinetic energy of the Auger electrons.] Since no signal to be assigned to Cu(0) is present in the Auger spectra, we can conclude the presence of Cu(I) oxide. This is further supported by electron diffraction studies (Fig. 9). Apart from substrate signals originating from TaN, the diffraction reflexes obtained are best fitted to Cu<sub>2</sub>O rather than CuO or Cu. However, the XPS core level spectra in Fig. 8 a also display signals at higher binding energies. In this respect, CuO would be expected at 933.2 eV [68] together with a satellite between 940 and 945 eV [68] and an Auger signal for the Cu LMM transition at 568.5 eV [69]. Apart from CuO, the Cu 2p satellite is also typical for Cu(OH)<sub>2</sub> together with a major signal at 935.1 eV [69] and an Auger peak at 570.4 eV (i.e., at a similar position as for Cu<sub>2</sub>O) [69]. Because the Cu 2p<sub>3/2</sub> core level signal as well as an Auger peak for CuO are not developed, we can further conclude that Cu(OH)<sub>2</sub> is present in addition to Cu<sub>2</sub>O. However, it is known from earlier studies by Baklanov et al. [71] that Cu samples exposed to air display the formation of a Cu hydroxide surface contamination. As we had also



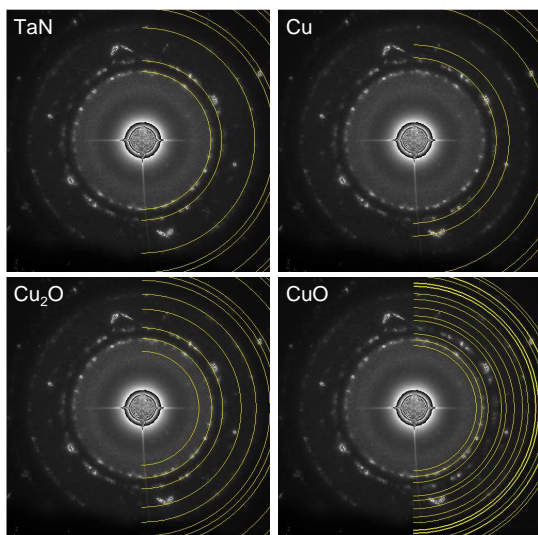


Fig. 9. Electron diffraction analysis of an ALD sample on TaN after cross-sectional TEM preparation. Apart from substrate signals originating from TaN, the diffraction reflexes obtained are best fitted to  $\text{Cu}_2\text{O}$  rather than  $\text{CuO}$  or  $\text{Cu}$ .

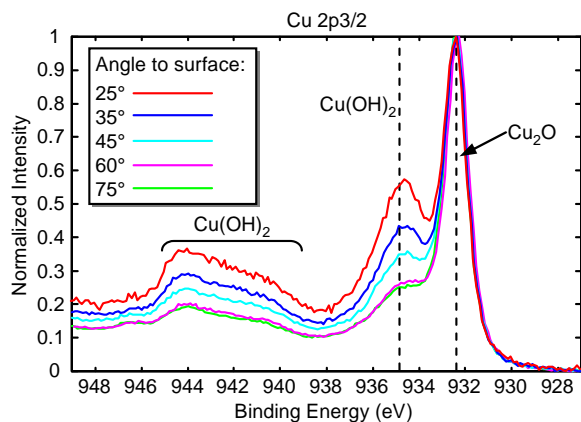


Fig. 10. Angle-resolved XPS analyses for ALD on TaN. The  $\text{Cu } 2p_{3/2}$  spectra suggest that  $\text{Cu}(\text{OH})_2$  is only present toward the sample surface, while in the bulk of the film  $\text{Cu}_2\text{O}$  dominates.

observed such effects on sputter-deposited  $\text{Cu}$  films, angle-resolved XPS analyses were carried out on the ALD samples in order to elucidate whether the  $\text{Cu}(\text{OH})_2$  results from a surface effect or if it is present throughout the entire ALD films. The respective spectra displayed in Fig. 10 suggest that  $\text{Cu}(\text{OH})_2$  is only present toward the sample surface, while in the bulk of the ALD films  $\text{Cu}_2\text{O}$  dominates as the  $\text{Cu}(\text{OH})_2$  peaks considerably decrease with increasing XPS take-off angle. Moreover, the sample grown at  $135^\circ\text{C}$  and examined 100 days later than the ones processed at  $115$  and  $125^\circ\text{C}$  exhibits a stronger transition toward  $\text{Cu}(\text{OH})_2$  shown both by the position of the  $\text{Cu } 2p_{3/2}$  signal as well as the broader peak in the  $\text{Cu}$  LMM spectrum (Fig. 8 a and b). This also points out that the effect is enhanced by prolonged exposure to ambient moisture.

The investigations further reveal the influence of TaN composition and processing temperature on the ALD film composition: While for the deposition on stoichiometric TaN

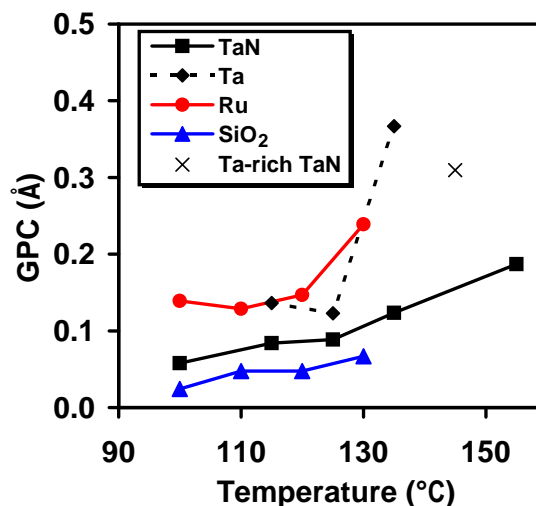


Fig. 11. GPC as a function of temperature for ALD on various substrate materials.

up to a temperature of  $135^\circ\text{C}$  only small or no temperature dependence (Fig. 11) and thus saturated growth are observed (Fig. 6), there is a considerable increase in the GPC seen at higher temperatures, resulting from beginning self-decomposition of the precursor and CVD growth modes setting in. This process is even more pronounced for the ALD on stronger metallic TaN, which is displayed by the data point marked with an  $\times$  in Fig. 11 and related to the XPS data of the dark blue, dotted curve in Fig. 8. In this respect, the Ta 4f spectrum in Fig. 8 c clearly shows the stronger metallic character of this tantalum nitride substrate as compared to the other TaN samples. Evidently, the stronger CVD effects in this case are due to enhanced precursor self-decomposition caused by the metallic Ta as theoretically predicted by Machado et al. [65], [66]. Similar effects were experienced earlier for the growth on stacks of Ta/TaN [64]. With respect to the chemical composition of the films grown under enhanced CVD conditions, one could expect metallic  $\text{Cu}$  to be present due to disproportionation of the precursor. However, the  $\text{Cu } 2p_{3/2}$  spectra together with the  $\text{Cu}$  LMM Auger data do not indicate this. Rather, they point to  $\text{Cu}_2\text{O}$  as in the other samples. This can either be explained by an immediate oxidation of any metallic  $\text{Cu}$  formed during the precursor pulses by the subsequent oxidation steps in the ALD process itself, or by an influence of the air exposure of the samples. Furthermore, the data suggest the formation of  $\text{Cu}(\text{OH})_2$  as observed before. However, due to the higher GPC, the ALD films were two to three times thicker compared to the samples grown between  $115$  and  $135^\circ\text{C}$ , so that the signals originating from  $\text{Cu}(\text{OH})_2$  formed on the surface appear considerably weaker in the normalized spectra.

In case of the ALD on Ru and  $\text{SiO}_2$  substrates, comparable results were achieved with respect to the chemical nature of the films. As depicted by Fig. 12, the fraction of  $\text{Cu}_2\text{O}$  was higher on  $\text{SiO}_2$ , whereas on Ru a greater tendency of  $\text{Cu}(\text{OH})_2$  formation than on  $\text{SiO}_2$  is seen. In addition, some  $\text{CuO}$  appears to be present on Ru, which is expressed by the broadening of

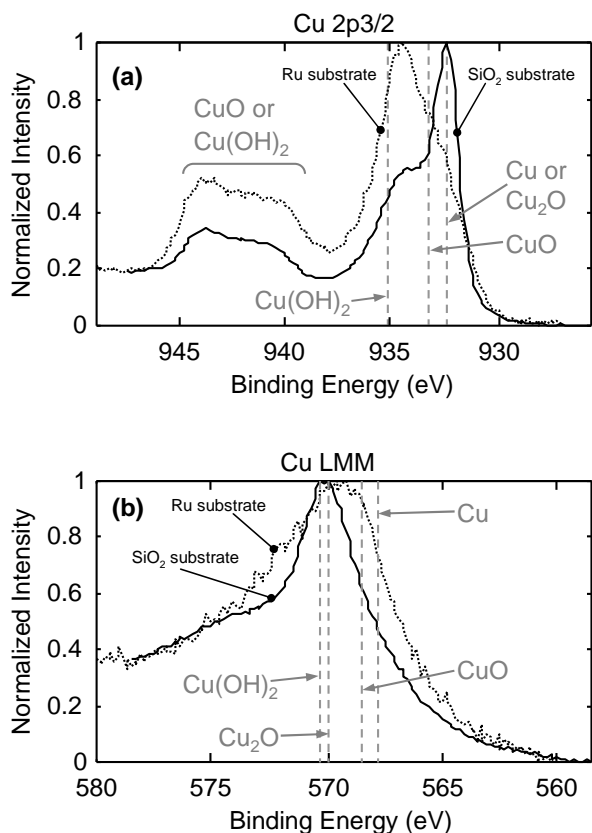


Fig. 12. (a) XPS Cu 2p<sub>3/2</sub> core level spectra and (b) Cu LMM Auger spectra for ALD samples on SiO<sub>2</sub> (solid line) and Ru (dotted line). The processes were carried out with precursor and purging steps of 5 s, and 11 s oxidation pulses at 120°C.

the peaks both in the Cu 2p<sub>3/2</sub> as well as in the Cu LMM spectra. This may be due to the ability of catalytic dissociation of O<sub>2</sub> on Ru [72] toward atomic oxygen, so that Cu<sub>2</sub>O formed during ALD could undergo an additional oxidative step, either during the ALD itself or afterward as a result of air exposure.

On all substrates investigated, nearly temperature-independent ALD growth was observed at least up to 120°C, as depicted by Fig. 11. In case of the Ta and Ru substrates, the GPC increased substantially above 130°C, due to beginning CVD growth modes. In contrast to the ALD on Ta where considerable formation of clusters was experienced, smooth films could be obtained on Ru also at the higher processing temperatures. Well-controlled ALD growth was also realized on Ru down to 100°C, giving an ALD window between 100 and 120°C. On TaN and SiO<sub>2</sub>, CVD effects were less pronounced, leading to more controlled ALD regimes along with an ALD window between 110 and 125°C. This is expressed in smooth films being deposited on silica, comparable to the ones obtained on TaN up to 135°C. As an example, Fig. 13 displays an AFM image of a 3 nm thick ALD film on silica, essentially replicating the surface roughness of the substrate, while the absolute values of the GPC on SiO<sub>2</sub> are considerably smaller compared to the ALD on the conductive substrates. These variations in the GPC may be due to varying density of adsorption sites and different modes of chemisorption depending on the substrate

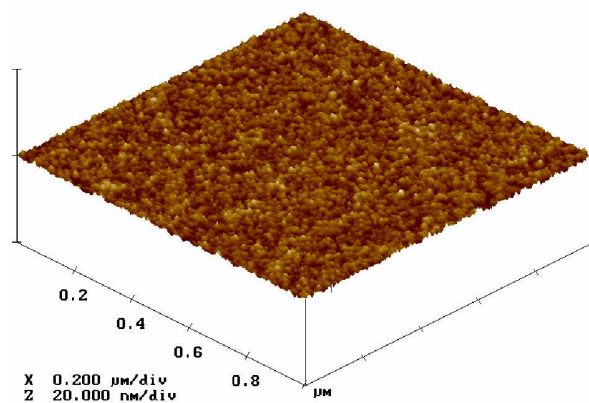


Fig. 13. AFM image of a 3 nm thick ALD copper oxide film grown on 300 nm thermal SiO<sub>2</sub>. An rms roughness of 0.25 nm was determined, very close to an as-grown SiO<sub>2</sub> film for which a value of 0.21 nm was measured.

[73]. However, one should expect similar growth once the substrate is covered with a monolayer of the growing film. In the current experiments, the composition of the films evidently also depends on the substrate as shown by the XPS investigations. This may be another reason for the variation of the GPC, although more detailed studies of the surface processes by in-situ methods need to be carried out for clarification.

For all substrates examined in this study, the adhesion of the ALD films grown with [(<sup>n</sup>Bu<sub>3</sub>P)<sub>2</sub>Cu(acac)] and wet oxygen was excellent. In no case did the films show signs of delamination. This is a considerable improvement compared to our earlier approach [64], where either O<sub>2</sub> or water vapor was used as oxidizing agent during ALD. Apart from the fact that in those cases no continuous films but only isolated clusters were grown on Ta, their adhesion to the substrate was so poor that they could be wiped off the wafer quite easily.

#### IV. SUMMARY

The thermal ALD growth of copper oxide films has been demonstrated on Ta, TaN, Ru, and SiO<sub>2</sub> substrates from bis(tri-*n*-butylphosphane)copper(I)acetylacetonate, [(<sup>n</sup>Bu<sub>3</sub>P)<sub>2</sub>Cu(acac)], and wet O<sub>2</sub>. Being nonfluorinated, the Cu precursor avoids a major source of adhesion problems well known from Cu CVD. Furthermore, it is available from less costly educts than its fluorinated counterparts. Nevertheless, the precursor is a liquid under standard conditions. This is another important fact for practical applications as solid-source precursors are prone to particle generation during deposition.

The ALD processes were carried out at moderate temperatures of well below 160°C, fulfilling a prerequisite to obtain ultrathin, continuous films and suppress agglomeration, which especially Cu is susceptible to. Temperature-independent growth regimes, essential for ALD, were found at least up to 120°C with GPC values of ~0.1 Å for the metallic substrates. The ALD window extends down to 100°C on Ru, while it was found to be somewhat narrower in case of TaN. However, saturated growth on TaN was still obtained at 135°C. Due to apparent precursor self-decomposition on Ta, a bimodal

growth was experienced, leading to the parallel formation of continuous films and isolated clusters. This effect was not observed on TaN up to  $\sim 130^\circ\text{C}$ , and neither did it appear for any of the depositions on Ru where very well-controlled growth regimes could be obtained. However, higher process temperature also led to the formation of clusters of  $\sim 20\text{ nm}$  on TaN and an increase of the GPC with temperature, being a clear sign of beginning CVD modes and thermal decomposition of the Cu precursor. In this respect, we observed that the degree of nitridation of the tantalum nitride underlayers considerably influences the growth of the films. This is in accordance with theoretical studies suggesting that metallic Ta leads to a strong decomposition tendency of metal-organic compounds [65]. On both Ta and TaN as well as on Ru, the ALD films showed very good adhesion in the tape test, most likely due to the absence of fluorine in the precursor, which is in strong contrast to the typical behavior of CVD grown Cu [30]–[32]. For a later application in ULSI metallization systems, this could open up an opportunity to reduce the liner thickness by avoiding the Ta layer between the TaN diffusion barrier and Cu conductor, and appears encouraging also with respect to novel liner materials, such as ruthenium.

Further ALD experiments under similar conditions on  $\text{SiO}_2$  yielded smooth, continuous films in all cases. No temperature dependence of the GPC was observed between  $110$  and  $120^\circ\text{C}$ . However, the absolute values of the growth rate were considerably lower than on the metallic substrates. The adhesion of the ALD grown films was excellent on silica as well.

The results appear promising for deposition processes of Cu nucleation layers applicable to ECD Cu metallization. For this purpose, reduction methods have to be found to convert the oxidic films into metallic Cu. Experiments with isopropanol and formic acid as the reducing agents gave very promising results and will be reported in due course.

#### ACKNOWLEDGMENTS

We thank Dr. Aslam Siddiqi (Gerhard-Mercator-Universität Duisburg, Germany) for vapor pressure measurements. The German Research Foundation (DFG) is acknowledged for funding obtained within the International Research Training Group 1215 "Materials and Concepts for Advanced Interconnects". The "Fonds der Chemischen Industrie" is also gratefully acknowledged for financial support.

#### REFERENCES

- [1] S. P. Murarka and S. W. Hymes, "Copper metallization for ULSI and beyond," *Crit. Rev. Solid-State Mat. Sci.*, vol. 20, pp. 87–124, 1995.
- [2] P. C. Andricacos, C. Uzoh, J. O. Dukovic, J. Horkans, and H. Deligianni, "Damascene copper electroplating for chip interconnections," *IBM J. Res. Develop.*, vol. 42, no. 5, pp. 567–574, 1998.
- [3] *ITRS International Technology Roadmap for Semiconductors 2007*. European Semiconductor Industry Association (ESIA), Japan Electronics and Information Technology Industries Association (JEITA), Korean Semiconductor Industry Association (KSIA), Taiwan Semiconductor Industry Association (TSIA), and United States Semiconductor Industry Association (SIA), 2007, available at <http://www.itrs.net/reports.html>.
- [4] H. Kim, "Atomic layer deposition of metal and nitride thin films: Current research efforts and applications for semiconductor device processing," *J. Vac. Sci. Technol. B*, vol. 21, no. 6, pp. 2231–2261, 2003.
- [5] H. Kim, "The application of atomic layer deposition for metallization of 65 nm and beyond," *Surf. Coat. Technol.*, vol. 200, pp. 3104–3111, 2006.

- [6] M. Leskelä and M. Ritala, "Atomic layer deposition chemistry: Recent developments and future challenges," *Angew. Chem. Int. Ed.*, vol. 42, pp. 5548–5554, 2003.
- [7] T. Suntola, "Atomic layer epitaxy," *Mater. Sci. Rep.*, vol. 4, pp. 261–312, 1989.
- [8] M. Ritala and M. Leskelä, "Atomic layer deposition," in *Handbook of Thin Film Materials. Vol. 1 – Deposition and Processing of Thin Films*, H. S. Nalwa, Ed. San Diego et al.: Academic Press, 2002, pp. 103–159.
- [9] T. Aaltonen, P. Alén, M. Ritala, and M. Leskelä, "Ruthenium thin films grown by atomic layer deposition," *Chem. Vap. Deposition*, vol. 9, no. 1, pp. 45–49, 2003.
- [10] T. Aaltonen, M. Ritala, T. Sajavaara, J. Keinonen, and M. Leskelä, "Atomic layer deposition of platinum thin films," *Chem. Mater.*, vol. 15, pp. 1924–1928, 2003.
- [11] T. Aaltonen, M. Ritala, V. Sammelselg, and M. Leskelä, "Atomic layer deposition of iridium thin films," *J. Electrochem. Soc.*, vol. 151, no. 8, pp. G489–G492, 2004.
- [12] O.-K. Kwon, J.-H. Kim, H.-S. Park, and S.-W. Kang, "Atomic layer deposition of ruthenium thin films for copper glue layer," *J. Electrochem. Soc.*, vol. 151, no. 2, pp. G109–G112, 2004.
- [13] T. Aaltonen, M. Ritala, and M. Leskelä, "ALD of rhodium thin films from  $\text{Rh}(\text{acac})_3$  and oxygen," *Electrochem. Solid-State Lett.*, vol. 8, no. 8, pp. C99–C101, 2005.
- [14] Y. Zhu, K. A. Dunn, and A. E. Kaloyeros, "Properties of ultrathin platinum deposited by atomic layer deposition for nanoscale copper-metallization schemes," *J. Mater. Res.*, vol. 22, no. 5, pp. 1292–1298, 2007.
- [15] S. K. Kim, S. Y. Lee, S. W. Lee, G. W. Hwang, C. S. Hwang, J. W. Lee, and J. Jeong, "Atomic layer deposition of Ru thin films using 2,4-(dimethylpentadienyl)(ethylcyclopentadienyl)Ru by a liquid injection system," *J. Electrochem. Soc.*, vol. 154, no. 2, pp. D95–D101, 2007.
- [16] C. Jezewski, W. A. Lanford, C. J. Wiegand, J. P. Singh, P.-I. Wang, J. J. Senkevich, and T.-M. Lu, "Inductively coupled hydrogen plasma-assisted Cu ALD on metallic and dielectric surfaces," *J. Electrochem. Soc.*, vol. 152, no. 2, pp. C60–C64, 2005.
- [17] L. Wu and E. Eisenbraun, "Hydrogen plasma-enhanced atomic layer deposition of copper thin films," *J. Vac. Sci. Technol. B*, vol. 25, no. 6, pp. 2581–2585, 2007.
- [18] A. Niskanen, A. Rahtu, T. Sajavaara, K. Arstila, M. Ritala, and M. Leskelä, "Radical-enhanced atomic layer deposition of metallic copper thin films," *J. Electrochem. Soc.*, vol. 152, no. 1, pp. G25–G28, 2005.
- [19] P. Mårtensson and J.-O. Carlsson, "Atomic layer epitaxy of copper on tantalum," *Chem. Vap. Deposition*, vol. 3, no. 1, pp. 45–50, 1997.
- [20] A. Johansson, T. Törndahl, L. M. Ottosson, M. Boman, and J.-O. Carlsson, "Copper nanoparticles deposited inside the pores of anodized aluminum oxide using atomic layer deposition," *Mater. Sci. Eng. C*, vol. 23, pp. 823–826, 2003.
- [21] T. Törndahl, M. Ottosson, and J.-O. Carlsson, "Growth of copper metal by atomic layer deposition using copper(I) chloride, water and hydrogen as precursors," *Thin Solid Films*, vol. 458, pp. 129–136, 2004.
- [22] J. A. Thornton, "Influence of substrate temperature and deposition rate on structure of thick sputtered Cu coatings," *J. Vac. Sci. Technol.*, vol. 12, no. 4, pp. 830–835, 1975.
- [23] M.-A. Nicolet, "Diffusion barriers in thin films," *Thin Solid Films*, vol. 52, pp. 415–443, 1978.
- [24] T. Hara, K. Sakata, A. Kawaguchi, and S. Kamijima, "Control of agglomeration on copper seed layer employed in the copper interconnection," *Electrochem. Solid-State Lett.*, vol. 4, no. 11, pp. C81–C84, 2001.
- [25] R. Saxena, M. J. Frederick, G. Ramanath, W. N. Gill, and J. L. Plawsky, "Kinetics of voiding and agglomeration of copper nanolayers on silica," *Phys. Rev. B*, vol. 72, p. 115425, 2005.
- [26] J. Wu, B. Han, C. Zhou, X. Lei, T. R. Gaffney, J. A. T. Norman, Z. Li, R. Gordon, and H. Cheng, "Density function theory study of copper agglomeration on the  $\text{WN}(001)$  surface," *J. Phys. Chem. C*, vol. 111, no. 26, pp. 9403–9406, 2007.
- [27] F. Fillot, Z. Tókei, and G. P. Beyer, "Surface diffusion of copper on tantalum substrates by Ostwald ripening," *Surf. Sci.*, vol. 601, pp. 986–993, 2007.
- [28] J. Huo, R. Solanki, and J. McAndrew, "Characteristics of copper films produced via atomic layer deposition," *J. Mater. Res.*, vol. 17, no. 9, pp. 2394–2398, 2002.
- [29] R. Solanki and B. Pathangey, "Atomic layer deposition of copper seed layers," *Electrochem. Solid-State Lett.*, vol. 3, no. 10, pp. 479–480, 2000.



- [30] S. Gandikota, S. Voss, R. Tao, A. Dobust, D. Cong, L.-Y. Chen, S. Ramaswami, and D. Carl, "Adhesion studies of CVD copper metallization," *Microelectron. Eng.*, vol. 50, pp. 547–553, 2000.
- [31] K. Weiss, S. Riedel, S. E. Schulz, M. Schwerd, H. Helneder, H. Wendt, and T. Gessner, "Development of different copper seed layers with respect to the copper electroplating process," *Microelectron. Eng.*, vol. 50, pp. 433–440, 2000.
- [32] S. Riedel, K. Weiss, S. E. Schulz, and T. Gessner, "Adhesion study on copper films deposited by MOCVD," in *Conference Proceedings Advanced Metallization Conference 1999 (AMC 1999)*, M. E. Gross, Ed., 2000, pp. 195–199.
- [33] P. Mårtensson and J.-O. Carlsson, "Atomic layer epitaxy of copper. Growth and selectivity in the Cu(II)-2,2,6,6-tetramethyl-3,5-heptanedionate/H<sub>2</sub> process," *J. Electrochem. Soc.*, vol. 145, no. 8, pp. 2926–2931, 1998.
- [34] P. Mårtensson, M. Juppo, M. Ritala, M. Leskelä, and J.-O. Carlsson, "Use of atomic layer epitaxy for fabrication of Si/TiN/Cu structure," *J. Vac. Sci. Technol. B*, vol. 17, no. 5, pp. 2122–2128, 1999.
- [35] B. S. Lim, A. Rahtu, J.-S. Park, and R. G. Gordon, "Synthesis and characterization of volatile, thermally stable, reactive transition metal amidinates," *Inorg. Chem.*, vol. 42, no. 24, pp. 7951–7958, 2003.
- [36] B. S. Lim, A. Rahtu, J.-S. Park, and R. G. Gordon, "Atomic layer deposition of transition metals," *Nature Mater.*, vol. 2, pp. 749–754, 2004.
- [37] Z. Li, S. T. Barry, and R. G. Gordon, "Synthesis and characterization of copper(I) amidinates as precursors for atomic layer deposition (ALD) of copper metal," *Inorg. Chem.*, vol. 44, no. 6, pp. 1728–1735, 2005.
- [38] Z. Li, R. G. Gordon, D. B. Farmer, Y. Lin, and J. Vlassak, "Nucleation and adhesion of ALD copper on cobalt adhesion layers and tungsten nitride diffusion barriers," *Electrochem. Solid-State Lett.*, vol. 8, no. 7, pp. G182–G185, 2005.
- [39] Z. Li, A. Rahtu, and R. Gordon, "Atomic layer deposition of ultrathin copper metal films from a liquid copper(I) amidinate precursor," *J. Electrochem. Soc.*, vol. 153, no. 11, pp. C787–C794, 2006.
- [40] Z. Li and R. G. Gordon, "Thin continuous and conformal copper films by reduction of atomic layer deposited copper nitride," *Chem. Vap. Deposition*, vol. 12, no. 7, pp. 435–441, 2006.
- [41] T. Törndahl, M. Ottosson, and J.-O. Carlsson, "Growth of copper(I) nitride by ALD using copper(II) hexafluoroacetylacetonate, water, and ammonia as precursors," *J. Electrochem. Soc.*, vol. 153, no. 3, pp. C146–C151, 2006.
- [42] H. Kim, H. B. Bhandari, S. Xu, and R. G. Gordon, "Ultrathin CVD Cu seed layer formation using copper oxynitride deposition and room temperature remote hydrogen plasma reduction," *J. Electrochem. Soc.*, vol. 155, no. 7, pp. H496–H503, 2008.
- [43] M. Utriainen, M. Kröger-Laukkanen, L.-S. Johansson, and L. Niinistö, "Studies of metallic thin film growth in an atomic layer epitaxy reactor using M(acac)<sub>2</sub> (M = Ni, Cu, Pt) precursors," *Appl. Surf. Sci.*, vol. 157, pp. 151–158, 2000.
- [44] J. Chae, J.-S. Park, and S.-W. Kang, "Atomic layer deposition of nickel by the reduction of preformed nickel oxide," *Electrochem. Solid-State Lett.*, vol. 5, no. 6, pp. C64–C66, 2002.
- [45] C. Lee and H.-H. Lee, "A potential novel two-step MOCVD of copper seed layers," *Electrochem. Solid-State Lett.*, vol. 8, no. 1, pp. G5–G7, 2005.
- [46] H. Kim, Y. Kojima, H. Sato, N. Yoshii, S. Hosaka, and Y. Shimogaki, "Thin and smooth Cu seed layer deposition using the reduction of low temperature deposited Cu<sub>2</sub>O," *Mater. Res. Soc. Symp. Proc.*, vol. 914, pp. 167–172, 2006.
- [47] H.-H. Lee, C. Lee, Y.-L. Kuo, and Y.-W. Yen, "A novel two-step MOCVD for producing thin copper films with a mixture of ethyl alcohol and water as the additive," *Thin Solid Films*, vol. 498, pp. 43–49, 2006.
- [48] O. Chyan, T. N. Arunagiri, and T. Ponnuswamy, "Electrodeposition of copper thin film on ruthenium. A potential diffusion barrier for Cu interconnects," *J. Electrochem. Soc.*, vol. 150, no. 5, pp. C347–C350, 2003.
- [49] T. P. Moffat, M. Walker, P. J. Chen, J. E. Bonevich, W. F. Egelhoff, L. Richter, C. Witt, T. Aaltonen, M. Ritala, M. Leskelä, and D. Josell, "Electrodeposition of Cu on Ru barrier layers for damascene processing," *J. Electrochem. Soc.*, vol. 153, no. 1, pp. C37–C50, 2006.
- [50] X.-P. Qu, J.-J. Tan, M. Zhou, T. Chen, Q. Xie, G.-P. Ru, and B.-Z. Li, "Improved barrier properties of ultrathin Ru film with TaN interlayer for copper metallization," *Appl. Phys. Lett.*, vol. 88, p. 151912, 2006.
- [51] S.-H. Kwon, O.-K. Kwon, J.-S. Min, and S.-W. Kang, "Plasma-enhanced atomic layer deposition of Ru–TiN thin films for copper diffusion barrier metals," *J. Electrochem. Soc.*, vol. 153, no. 6, pp. G578–G581, 2006.
- [52] C.-W. Chen, J. S. Chen, and J.-S. Jeng, "Improvement on the diffusion barrier performance of reactively sputtered Ru–N film by incorporation of Ta," *J. Electrochem. Soc.*, vol. 155, no. 6, pp. H438–H442, 2008.
- [53] S. Kumar, H. L. Xin, P. Ercius, D. A. Muller, and E. Eisenbraun, "ALD growth of a mixed-phase novel barrier for seedless copper electroplating applications," in *Proc. IEEE 2008 International Interconnect Technology Conference (IITC 2008)*, 2008, pp. 96–98.
- [54] J. P. Chu and C. H. Lin, "High performance Cu containing Ru or RuN<sub>x</sub> for barrierless metallization," in *Proc. IEEE 2008 International Interconnect Technology Conference (IITC 2008)*, 2008, pp. 25–27.
- [55] K. Mori, K. Ohmori, N. Torazawa, S. Hirao, S. Kaneyama, H. Korogi, K. Maekawa, S. Fukui, K. Tomita, M. Inoue, H. Chibahara, Y. Imai, N. Suzumura, K. Asai, and M. Kojima, "Effects of Ru–Ta alloy barrier on Cu filling and reliability for Cu interconnects," in *Proc. IEEE 2008 International Interconnect Technology Conference (IITC 2008)*, 2008, pp. 99–101.
- [56] H.-K. Shin, M.-J. Hampden-Smith, E. N. Duesler, and T. T. Kodas, "The chemistry of copper(I) β-diketonate compounds. Part V. syntheses and characterization of (β-diketonate)CuL<sub>n</sub> species where L = PBU<sub>3</sub>, PPh<sub>3</sub>, and PCy<sub>3</sub>; n = 1 and 2; crystal and molecular structures of (acac)Cu(PCy<sub>3</sub>), (tfac)Cu(PCy<sub>3</sub>), (hfac)Cu(PCy<sub>3</sub>), and (hfac)Cu(PCy<sub>3</sub>)<sub>2</sub>," *Can. J. Chem.*, vol. 70, pp. 2954–2966, 1992.
- [57] Y.-Z. Shen, M. Leschke, S. E. Schulz, R. Ecke, T. Gessner, and H. Lang, "Synthesis of tri-*n*-butylphosphine copper(I) β-diketonates and their use in chemical vapour deposition of copper," *Chin. J. Inorg. Chem.*, vol. 20, no. 11, pp. 1257–1264, 2004.
- [58] J. A. T. Norman, B. A. Muratore, P. N. Dyer, D. A. Roberts, and A. K. Hochberg, "New OMCVD precursors for selective copper metallization," *J. Phys. IV*, vol. 2, pp. 271–278, 1991.
- [59] S. K. Reynolds, C. J. Smart, E. F. Baran, T. H. Baum, C. E. Larson, and P. J. Brock, "Chemical vapor deposition of copper from 1,5-cyclooctadiene copper(I)hexafluoroacetylacetonate," *Appl. Phys. Lett.*, vol. 59, no. 18, pp. 2332–2334, 1991.
- [60] R. Teghil, D. Ferro, L. Bencivenni, and M. Pelino, "A thermodynamic study of the sublimation processes of aluminum and copper acetylacetonates," *Thermochim. Acta*, vol. 44, pp. 213–222, 1981.
- [61] J. Röber, C. Kaufmann, and T. Gessner, "Structure and electrical properties of thin copper films deposited by MOCVD," *Appl. Surf. Sci.*, vol. 91, pp. 134–138, 1995.
- [62] H. Wolf, J. Röber, S. Riedel, R. Streiter, and T. Gessner, "Process and equipment simulation of copper chemical vapor deposition using Cu(hfac)vtms," *Microelectron. Eng.*, vol. 45, pp. 15–27, 1999.
- [63] M. Böhme, "Design of a process controller for atomic layer deposition," *Student research report (in German)*, Chemnitz University of Technology, 2005, available at: <http://archiv.tu-chemnitz.de/pub/2005/0191>.
- [64] T. Waechter, S. Oswald, A. Pohlers, S. Schulze, S. E. Schulz, and T. Gessner, "Copper and copper oxide composite films deposited by ALD on tantalum-based diffusion barriers," in *Conference Proceedings AMC XXIII, Advanced Metallization Conference 2007*, A. J. McKerrow, Y. Shacham-Diamond, S. Shingubara, and Y. Shimogaki, Eds. Warrendale, PA: Materials Research Society, 2008, pp. 23–29.
- [65] E. Machado, M. Kaczmarek, P. Ordejón, D. Garg, J. Norman, and H. Cheng, "First-principles analyses and predictions on the reactivity of barrier layers of Ta and TaN toward organometallic precursors for deposition of copper films," *Langmuir*, vol. 21, pp. 7608–7614, 2005.
- [66] E. Machado, M. Kaczmarek, B. Braida, P. Ordejón, D. Garg, J. Norman, and H. Cheng, "Interaction of copper organometallic precursors with barrier layers of Ti, Ta and W and their nitrides: a first-principles molecular dynamics study," *J. Mol. Model.*, vol. 13, pp. 861–864, 2007.
- [67] J. Pinkas, J. C. Huffman, D. W. Baxter, M. H. Chisholm, and K. G. Caulton, "Mechanistic role of H<sub>2</sub>O and the ligand in the chemical vapor deposition of Cu, Cu<sub>2</sub>O, CuO, and Cu<sub>3</sub>N from bis(1,1,1,5,5,5-hexafluoropentane-2,4-dionato)copper(II)," *Chem. Mater.*, vol. 7, pp. 1589–1596, 1995.
- [68] J. Ghijsen, L. H. Tjeng, J. van Elp, H. Eskes, J. Westerink, G. A. Sawatzky, and M. T. Czyzyk, "Electronic structure of Cu<sub>2</sub>O and CuO," *Phys. Rev. B*, vol. 38, no. 16, pp. 11 322–11 330, 1988.
- [69] N. S. McIntyre, S. Sunder, D. W. Shoesmith, and F. W. Stanchell, "Chemical information from XPS—applications to the analysis of electrode surfaces," *J. Vac. Sci. Technol.*, vol. 18, no. 3, pp. 714–721, 1981.
- [70] S. W. Gaarenstroom and N. Winograd, "Initial and final state effects in the ESCA spectra of cadmium and silver oxides," *J. Chem. Phys.*, vol. 67, no. 8, pp. 3500–3506, 1977.
- [71] M. R. Baklanov, D. G. Shamiryan, Z. Tókei, G. P. Beyer, T. Conard, S. Vanhaelemeersch, and K. Maex, "Characterization of Cu surface cleaning by hydrogen plasma," *J. Vac. Sci. Technol. B*, vol. 19, no. 4, pp. 1201–1211, 2001.

- [72] M. C. Wheeler, D. C. Seets, and C. B. Mullins, “Kinetics and dynamics of the initial dissociative chemisorption of oxygen on Ru(001),” *J. Chem. Phys.*, vol. 105, no. 4, pp. 1572–1583, 1996.
- [73] R. L. Puurunen, “Surface chemistry of atomic layer deposition: A case study for the trimethylaluminum/water process,” *J. Appl. Phys.*, vol. 97, p. 121301, 2005.